JOURNAL OF MATERIALS SCIENCE 8 (1973) 1616–1624

Effects of prior plastic deformation on the martensitic transformation in oriented single crystals of Au-47.5 at.% Cd

M. L. GREEN*, M. S. WALD, K. MUKHERJEE
Polytechnic Institute of Brooklyn, Brooklyn, New York, USA

Oriented single crystal samples of β phase Au-47.5 at. % Cd were progressively compressed along [110], [111] and [112] axes, causing each sample to deform with a different {110} ⟨001⟩ slip multiplicity and, therefore, develop a different defect substructure. The effects of the existing substructure upon subsequent martensite and reverse transformation were studied as a function of deformation for each sample, using a resistance technique.

It was observed that for small amounts of reduction in thickness ($\leqslant 5\%$), the greater the work-hardening rate associated with deformation, the greater the enhancement of the martensite nucleation (increase in M_s temperature). It is suggested that {110} ⟨1$\bar{1}$0⟩ slip band intersections, produced during prior deformation, are responsible for this enhancement. For larger amounts of reduction in thickness ($>5\%$), for the [110] and [111] samples, martensite nucleation becomes less enhanced, and finally inhibited. Deformation of the [112] sample has little effect upon martensite nucleation behaviour for any amount of reduction in thickness, because it undergoes almost single slip and presumably, few slip band intersections are formed. There is no apparent correlation between prior deformation and A_s temperature.

The greater the work-hardening rate associated with deformation, the greater the increase in difficulty of propagation of both the martensite and the austenite as a function of reduction in thickness. Defect pinning of the transformation interface is suggested as a possible mechanism to explain this observation. Also, practically the same increase in difficulty of propagation is observed for the A → M and M → A transformations for any sample, suggesting that the defects responsible for pinning are not erased after the two cycles that the sample is subjected to during testing.

1. Introduction

Much deformation work has been done on ferrous as well as nonferrous martensitic systems. Scheil [1] proposed that martensitic transformation and slip were competitive processes for producing strain in a lattice. He observed that the application of stress raised the transformation temperature above the M_S temperature. However, above a temperature which he called M_d, no further transformation was induced by the application of stress. McReynolds [2] extended Scheil's work and found that $M_d \sim (M_S + 75°C)$ for Fe-Ni alloys. In general, the effect of deformation has been interpreted as the creation of strain inhomogeneities which act as preferential sites for the nucleation of martensite. Increases in the M_S temperatures caused by deformation served as indications that nucleation was facilitated [1-6]. However, it has been reported that large

*Present address: Bell Laboratories, Murray Hill, New Jersey.
Submitted in partial fulfilment of the requirements for the degree of Master of Science at the Polytechnic Institute of Brooklyn by Martin L. Green.

amounts of plastic deformation suppress the M_S temperature as well as the amount of martensite formed [2-7].

In this work, single crystal samples of Au-47.5 at. %Cd, an alloy whose β (cubic) to β' (orthorhombic) martensitic transformation is well characterized [5], were oriented and progressively compressed along [110], [111] and [112] axes. Since equiatomic AuCd displays a $\{110\}\langle 001\rangle$ slip mode [8], compression along these axes should lead to a different $\{110\}\langle 001\rangle$ slip multiplicity for each sample. Because of this, each sample is expected to develop a different defect substructure. That is, for a given amount of deformation, the total number of defect arrays (henceforth called slip band intersections) should be greater the greater the slip multiplicity associated with deformation along a particular axis. At various levels of deformation, the effects of the different substructures upon the nucleation and propagation of the martensite transformation and the reverse transformation were studied using a resistance technique.

2. Experimental procedure

To prepare the Au-47.5 at. % Cd alloy, appropriate amounts of 99.999% Au and Cd were placed in a quartz tube previously cleaned with HF, evacuated to 10^{-6} μm, backfilled with purified argon to a pressure of 200 μm and sealed. The alloy was melted in the tube and agitated to ensure homogeneity. It was then placed in a resistance furnace, brought up to a temperature of 800°C and directionally solidified at the rate of 9.5 cm h^{-1} to yield a single crystal.

The crystal was heated into the β phase (M_S = martensite start = 55 °C ± 1 °C, A_S = austenite start = 71°C ± 1°C) with a hot air gun and its orientation determined by the Laüe back reflection technique. Suitably oriented and shaped samples were cut from the bulk crystal using an MRL Servomet spark machine. Typical sample dimensions were 1 cm × 0.25 cm × 0.25 cm. Initially, each sample was cycled several times through the forward and reverse transformation to stabilize the resistance hysteresis loop.

Samples to be deformed along [110], [111] and [112] axes were heated into the β phase (~ 100°C) with a hot air gun and compressed on an Instron mechanical tester. Nakanishi *et al* [9] stressed β phase Au-47.5 at. % Cd at a temperature just a few degrees above the M_S temperature and observed jagged yielding which they attributed to stress induced transformation. No anomalies were observed in the stress-strain behaviour of any of the samples tested in this work and it is, assumed, therefore, that no martensite was induced during deformation at 100°C. Each sample was deformed to approximately 5, 10 and 20% reduction in thickness. After each level of deformation, the samples were cooled to ambient temperature and transferred to the resistance measurement equipment. Therefore, in measuring the resistance, a first cycle orthorhombic to cubic transformation and a second cycle cubic to orthorhombic transformation were observed.

The resistance apparatus used was based on a four point technique. Four stainless steel wires were strung over the sample, which rested on top of a 60 cm quartz rod. The wires were tensioned by a collar at the bottom of the rod and led through a vacuum plate to the external circuitry. The quartz rod was immersed in a nichrome wound quartz tube furnace, pumped down to a pressure of 20 μm and back-filled with argon. The temperature was monitored by a Pt-Pt 10% Rh thermocouple placed in contact with the sample. Temperature readings were accurate to ± 0.1°C. During a typical resistance hysteresis loop determination, a sample was cycled from ambient temperature to 100°C and back, at heating and cooling rates of 2°C min^{-1}. Current and voltage measurements were obtained on PAR HR-8 phase locked amplifiers. Fluctuations in sample current were automatically compensated for in the external circuitry. For typical sample current and sample dimensions, the voltage drop in the sample was about 50 μV, which was two orders of magnitude greater than the noise level. A large fraction of the sample voltage (~ 75%) could be suppressed with external circuitry, permitting changes in resistance of less than 1 part in 10^3 to be seen. Because the samples tended to be slightly irregular in shape after deformation, errors were introduced into the absolute values of the resistivities; therefore, resistance, rather than resistivity, was determined. However, for an undeformed (annealed) sample, the value of resistivity (9.5 μΩ-cm at 60°C), agreed with the value in the literature [5]. The current into the sample, voltage drop in the sample and temperature of the sample were taken automatically about every half degree and stored on tape for computer processing.

3. Results

3.1. Mechanical behaviour of β phase Au-47.5 at. % Cd

An understanding of the mechanical behaviour of the β phase is essential for a meaningful interpretation of the results. Based on Rachinger and Cottrell's [8] observation that equiatomic AuCd displays a {110} ⟨001⟩ slip mode, samples compressed along [110], [111] and [112] axes should have slip multiplicities (based on equal Schmid factors) as indicated in Table I. Two-surface trace analysis was used to deduce the observed slip multiplicity. The observed slip traces were distributed evenly over the surfaces of the samples at about 20% reduction in thickness, indicating that homogeneous deformation on an optical microscopic level had occurred.

Only the [111] sample deformed with the predicted slip multiplicity. The [110] sample, which was in actuality oriented slightly away from [110], deformed on two systems rather than the four that were predicted. The two very weak systems observed on the [112] sample were difficult to notice even after 22.3% reduction in thickness, suggesting that slip occurred predominantly on the one {110} plane that is observed. Most important is the fact that the observed work-hardening rates are consistent with the assessment that they are related to the total number of slip band intersections, which is likely to be greater the greater the observed slip multiplicity.

3.2. Effects of prior deformation

In Fig. 1 resistance hysteresis loops for the [111] sample for the annealed condition and for 4.3% reduction in thickness are plotted, illustrating the characteristic change in shape of the loop that occurs upon deformation. The overall increase in resistance observed after deformation is owing, in part, to the decreased cross-sectional area of the sample. Although resistivity, which is independent of sample geometry, would have been a more revealing quantity to plot, it could not be accurately determined for these samples, for the reason mentioned earlier.

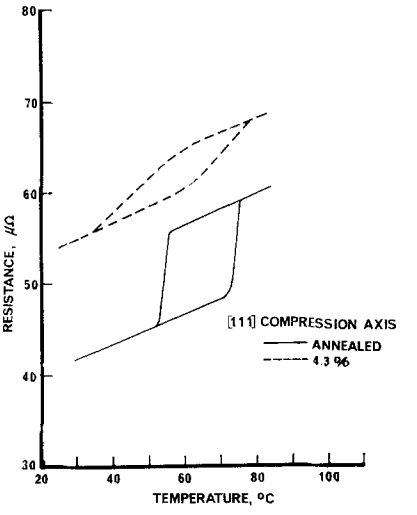

Figure 1 Annealed and deformed (4.3% reduction in thickness) resistance hysteresis loops for the [111] sample. The overall increase in resistance observed after deformation is due, in part, to the decreased cross-sectional area of the sample.

All deformation was carried out in the β phase. For discussion purposes, the β phase will be called the austenite (A) phase and the orthorhombic phase, β', the martensite (M) phase. One can study the various trends observed in the hysteresis loops by defining the following quantities, illustrated in Fig. 2.

M_S, A_S: the temperatures corresponding to the points of deviation of tangents drawn to the upper (dR_A/dT) and the lower (dR_M/dT) segments of the loop, respectively.

$\theta_{A\rightarrow M}$, $\theta_{M\rightarrow A}$: the angles made by the left and right segments of the loop and the horizontal, respectively. The inverse slope of either of these segments, dT/dR or (cot θ), is a measure of the difficulty involved in propagating the trans-

TABLE I Mechanical behaviour of β phase Au-47.5 at. % Cd

Compression axis	Calculated slip multiplicity*	Observed slip multiplicity	Work-hardening rate† ($MNm^{-2} \times 10^{-3}$)
[112]	1	1{110} plus two very weak traces	0.26
[110]	4	2{110}	1.26
[111]	3	3{110}	1.72

*Based on equal Schmid factors for a {110} ⟨001⟩ slip mode.
†Average work-hardening rate for the three levels of deformation.

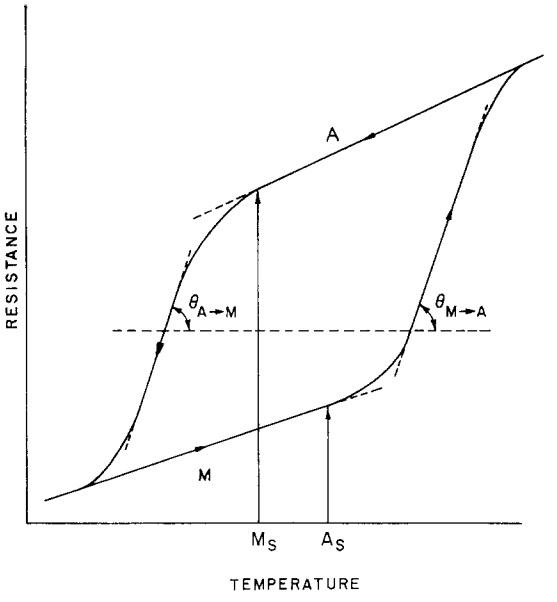

Figure 2 Typical resistance hysteresis loop illustrating the parameters defined in the text.

formation interface. The greater dT/dR, the greater the difficulty of propagation.

3.2.1. Effects of prior deformation upon the nucleation of martensite and austenite

In Fig. 3, the change in M_S temperature owing to prior deformation is plotted versus % reduction in thickness for [1 1 0], [1 1 1] and [1 1 2] samples. For small amounts of reduction in thickness ($\leqslant$ 5%), for all sample orientations, there is excellent correlation between the work-hardening rate and the increase in the M_S temperature (enhancement of martensite nucleation). Deformation of the [1 1 2] sample, which exhibits almost single slip and consequently, the lowest work-hardening rate, has very little effect on the M_S temperature. The [1 1 0] and [1 1 1] samples, which exhibited higher-work hardening rates, show correspondingly higher peak increases in the M_S temperature. For larger amounts of reduction in thickness (> 5%) for the [1 1 0] and [1 1 1] samples, the nucleation of martensite

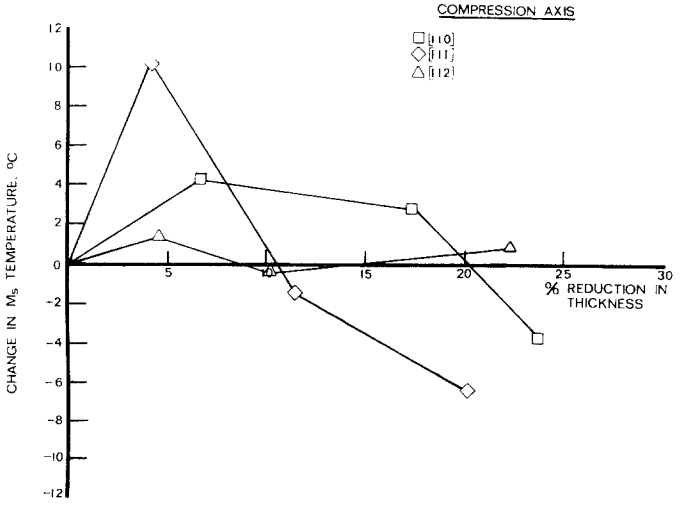

Figure 3 Change in M_S temperature as a function of reduction in thickness for [1 1 0], [1 1 1] and [1 1 2] samples.

becomes less enhanced until it is finally inhibited. Deformation of the [112] sample has very little effect on the M_s temperature for any amount of reduction in thickness.

The change in A_s temperature owing to prior deformation for [110], [111] and [112] samples is tabulated in Table II.

There is no apparent correlation between prior deformation and the A_s temperature. Furthermore, there is no apparent correlation between the changes in the M_s temperature and the changes in the A_s temperature after deformation.

3.2.2. Effects of prior deformation upon the propagation of martensite and austensite

In Fig. 4, $dT/dR_{A\rightarrow M}$ and $dT/dR_{M\rightarrow A}$ ($\cot\theta_{A\rightarrow M}$ and $\cot\theta_{M\rightarrow A}$) are plotted versus % reduction in thickness for [110], [111] and [112] samples. Two separate observations can be drawn from this figure. Firstly, for each sample orientation, one observes almost the same characteristic change in both $dT/dR_{A\rightarrow M}$ and $dT/dR_{M\rightarrow A}$ with reduction in thickness. Secondly, for any amount of reduction in thickness, the higher the work-hardening rate associated with deformation of a sample, the more difficult the propagation of the $A\rightarrow M$ or $M\rightarrow A$ transformation (that is, the higher $dT/dR_{A\rightarrow M}$ or $dT/dR_{M\rightarrow A}$) in that sample.

In addition, there is good agreement between Figs. 3 and 4 for small amounts of reduction in thickness ($\leqslant 5\%$). Deformation along those crystallographic axes that results in large peak increases in M_s temperature, such as [110] and [111], also results in correspondingly large increases in the difficulty of propagation of the martensite and the austenite. The agreement is also good for the [112] sample, where the degree of martensite nucleation enhancement is small. However, for larger amounts of reduction in thickness ($> 5\%$), the difficulty of propagation continues to increase, whereas the nucleation of martensite becomes less enhanced and finally, inhibited.

Attempts were made to relate the resistance

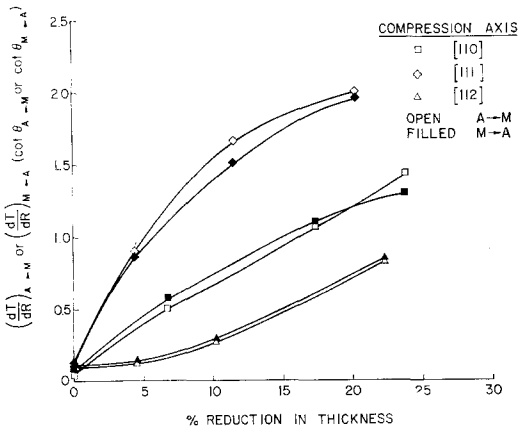

Figure 4 $dT/dR_{A\rightarrow M}$ and $dT/dR_{M\rightarrow A}$ as a function of reduction in thickness for [110], [111] and [112] samples.

gap of a deformed sample, $(R_A - R_M)_{def}$, to the degree of completion of transformation, by assuming that the resistance gap for the same sample in the annealed condition $(R_A - R_M)_{ann}$, represented 100% transformation in both directions. The correlation is at best only a qualitative one, because there are unknown contributions to the resistance of the deformed sample owing to deformation induced defects [10] and deformation induced disorder [11]. However, X-ray diffraction of the deformed samples indicated that some austenite phase was retained at room temperature, demonstrating that transformation was not complete, at least in the forward direction. No retained austenite was observed in any of the annealed samples at room temperature. In addition, all of the martensite formed in these samples was of the orthorhombic type.

4. Discussion of results

4.1. Changes in M_s and A_s temperatures

Figs. 3 and 4 reveal the following general trends: the peak increases in M_s temperature and the relative increases in the difficulty of propagation are both greater the greater the work-hardening rate associated with deformation. This seems to

TABLE II Effect of prior deformation on the A_s temperature

[110] % reduction in thickness	ΔA_s	[111] % reduction in thickness	ΔA_s	[112] % reduction in thickness	ΔA_s
6.7	−2.5	4.3	−11.4	4.5	12.9
17.4	−10.2	11.5	−10.7	10.2	10.9
23.8	−10.1	20.2	−13.7	22.3	7.6

indicate that the nucleation of shear martensite and the propagation of martensite and austenite in deformed Au-47.5 at. % Cd are defect controlled processes, since the greater the work-hardening rate, the greater the total number of slip band intersections, for a given amount of reduction in thickness.

The results of both theoretical and experimental deformation studies as a function of orientation for martensitic systems suggests that martensite transformation behaviour is dependent not only on the total number, but also the character of slip band intersections [12-17]. It is suggested in the present study that the observed enhancement of martensite nucleation can be explained in terms of slip band intersections of a particular character, because of the well-defined crystallography of the martensitic transformation in Au-47.5 at. % Cd.

One possible mechanism for the observed enhancement of martensite nucleation would be the production of slip band intersections of the type $\{1\,1\,0\}\langle 1\,\bar{1}\,0\rangle$ during prior deformation. The martensitic transformation in Au-47.5 at. % Cd occurs by a $\{1\,1\,0\}\langle 1\,\bar{1}\,0\rangle$ shear mode and, therefore, these slip band intersections (henceforth called slip nuclei) should act as preferential sites for martensite nucleation. One can easily show that $\{1\,1\,0\langle 1\,\bar{1}\,0\rangle$ slip nuclei can occur as a result of the intersection of two $\{1\,1\,0\}\langle 0\,0\,1\rangle$ slip bands; furthermore, the number of $\{1\,1\,0\}\langle 1\,\bar{1}\,0\rangle$ slip nuclei turns out to be greater the greater the $\{1\,1\,0\}\langle 0\,0\,1\rangle$ slip multiplicity, and, therefore, the greater the work-hardening rate, associated with deformation.*

This mechanism explains the results of Fig. 3. For small amounts of reduction in thickness ($\leqslant 5\%$), the greater the work-hardening rate associated with deformation, the greater the enhancement of martensite nucleation. For the [1 1 2] sample, which exhibited only one major $\{1\,1\,0\}\langle 0\,0\,1\rangle$ slip system, no $\{1\,1\,0\}\langle 1\,\bar{1}\,0\rangle$ slip nuclei, and therefore no martensite nucleation enhancement was expected. The small enhancement peak that is observed for this sample is probably owing to other slip nuclei between the one $\{1\,1\,0\}\langle 0\,0\,1\rangle$ system and the two very weak systems that are observed. The low work-hardening rate exhibited by the [1 1 2] sample is consistent with this suggestion.

For larger amounts of reduction in thickness ($> 5\%$), the [1 1 2] sample continues to have only a small effect on martensite nucleation behaviour, probably because of the low probability of forming slip nuclei. However, for the [1 1 0] and [1 1 1] samples, nucleation of martensite becomes less enhanced and finally, inhibited. This fact is interesting and in agreement with the literature [2, 4]. Many of the potential sites for martensite nucleation may become tangled with increasing reduction in thickness and, therefore, even though martensite nucleation may continue to be enhanced for larger amounts of reduction in thickness, the difficulty of propagation is so great that a deviation from the linear slope dR_A/dT (defined as the M_S temperature in this study) may not be seen until a lower temperature. This, the authors believe, is the reason for the decreased enhancement and finally, inhibition, of martensite nucleation that is observed with increasing reduction in thickness. Furthermore, this means that the M_S temperature, as defined in this study, is a better indication of martensite nucleation behaviour for small amounts of reduction in thickness ($\leqslant 5\%$), where difficulty of propagation (see Fig. 4) is not a severe problem, than for larger amounts of reduction in thickness ($> 5\%$).

Unfortunately, the authors have no way of effectively explaining the changes in the A_S temperatures (Table II) that are observed after deformation. Obviously, the deformation induced defects are playing some role in the M $\rightarrow$ A transformation, since changes of up to 13.7°C are observed.

One can suggest two reasons, however, to try to explain why there need not be any correlation between the M_S and the A_S temperatures. Firstly, the A $\rightarrow$ M transformation is a single crystalline to polycrystalline transformation, because transformation will occur upon several habits in a deformed crystal of austenite. The M $\rightarrow$A transformation, however, is a polycrystalline to single crystalline transformation, and the effect of the the constraints of the neighbouring regions of martensite will undoubtedly have some effect on the A_S temperature, although the nature of the effect will depend upon the various orientation relationships among these regions. Naturally, this constraint factor will not play a role in the A $\rightarrow$ M transformation. McReynolds [2] mentions the constraint factor in explaining the variation of M_S temperature with austenite

*See Appendix.

grain size. Secondly, the A → M transformation is a high to low symmetry transformation (cubic → orthorhombic), whereas the opposite is true for the M → A transformation. Therefore, the transformation shears for the M → A transformation are probably different than those for the A → M transformation [5]. For that reason, the deformation induced defects probably play a different role in the M → A transformation.

The mechanism of the M → A transformation is apparently more involved than the A → M transformation and the authors do not have enough facts to explain the A_S temperature data. Only limited work has been done on the M → A transformation as compared to the A → M transformation, for any system [5-7].

4.2. Changes in $(dT/dR)_{A\to M}$ and $(dT/dR)_{M\to A}$

From Fig. 4 it is seen that the greater the work-hardening rate associated with deformation, the greater the increase in the difficulty of propagation of the martensite and the austenite, as a function of reduction in thickness. This suggests that the transformation interfaces are being physically blocked by deformation induced defects, because the greater the work-hardening rate, the greater the total number of slip band intersections produced, for any amount of reduction in thickness.

For small amounts of reduction in thickness ($\leqslant 5\%$), the correlation between Figs. 3 and 4 is good. That is, the greater the peak enhancement of martensite nucleation, the greater the increase in the difficulty of propagation. This relationship is to be expected since the number of $\{1\,1\,0\}\langle 1\,\bar{1}\,0\rangle$ slip nuclei, which are postulated to cause enhancement, increases as the work-hardening rate, and, therefore, as the total number of slip nuclei increases. For larger amounts of reduction in thickness ($> 5\%$), the difficulty of propagation continues to increase, indicating that slip nuclei continue to be created in the sample, whereas the enhancement of martensite nucleation decreases. This apparent breakdown in the correlation between Figs. 3 and 4 is a result of the increased difficulty of propagation being reflected in the measured M_S temperature, as discussed earlier.

The fact that practically the same behaviour is observed for the A → M and M → A transformations (Fig. 4) as a function of reduction in thickness for any sample is interesting. Since martensite and austenite are created by the forward and backward motion of the same interface [5] it is probable that the deformation induced defects that are responsible for blocking the interface are not erased to any great extent by the moving interface after the two cycles that the sample is subjected to in this study. If many defects were erased, the difficulty of propagation of any transformation should be less than for the previous transformation: this is not observed in Fig. 4. The effects of repeated cycling upon the deformation induced defects have not been studied here.

The time required for resistance loop measurement was a constant; therefore, one should expect a correlation between the difficulty of propagation and the degree of completion of transformation for a given sample. Although X-ray diffraction does reveal that transformation is incomplete in the deformed samples, it is not possible to be more quantitative, because single crystalline samples, even after deformation, tend to be highly textured, and do not easily lend themselves to reliable measurement of Bragg peak intensities.

Ferraglio and Mukherjee [18] saw evidence of interface pinning by defects in splat-cooled films of Au-47.5 at. % Cd using transmission electron microscopy. The same mechanism is probably responsible for the increased difficulty of propagation and the corresponding decreased degree of transformation, that is observed upon deformation. This mechanism would be sensitive to the total number of slip band intersections in the sample and would explain the dependence on work-hardening rate and amount of reduction in thickness that is observed in Fig. 4, for the various samples.

5. Summary and conclusions

1. The fact that the peak increases in M_S temperature and the increases in the difficulty of propagation of the martensite and the austenite are both greater the greater the work-hardening rate associated with deformation suggests that nucleation of the martensite and propagation of the martensite and the austenite in deformed Au-47.5 at. % Cd are defect controlled processes.

2. Because of the well defined crystallography of the martensitic transformation in Au-47.5 at. % Cd, it is suggested that slip nuclei having the character $\{1\,1\,0\}\langle 1\,\bar{1}\,0\rangle$, which can form through the intersection of two $\{1\,1\,0\}\langle 0\,0\,1\rangle$ slip bands, are responsible for the enhancement of martensite nucleation since they provide preferential sites

for transformation shearing to occur. Furthermore, the number of $\{110\}\langle 1\bar{1}0\rangle$ slip nuclei will be greater the greater the $\{110\}\langle 001\rangle$ slip multiplicity. This mechanism explains why, for small amounts of reduction in thickness ($\leqslant 5\%$), the greater the work-hardening rate, the greater the enhancement of martensite nucleation (Fig. 3).

3. For larger amounts of reduction in thickness ($> 5\%$), for the [110] and [111] samples, martensite nucleation becomes less enhanced and finally inhibited. It is suggested that nucleation probably continues to be enhanced; however, because of the definition of the M_S temperature used in this study, difficulty of propagation is reflected in the M_S temperature, causing it to decrease with increasing amount of reduction in thickness. Compression of the [112] sample has little effect on martensite nucleation for any amount of reduction in thickness, probably because of the low probability of producing potential slip nuclei.

4. There is no apparent correlation between prior deformation and the A_S temperature. The authors are unable to explain this result to their satisfaction. Furthermore, there is no apparent correlation between the M_S and the A_S temperatures. It is suggested that there need not be a correlation, based on the following reasons: the $M \rightarrow A$ transformation is constrained by neighbouring areas of martensite of different habit, and the deformation induced defects play a different role in the $M \rightarrow A$ transformation because the transformation shears involved are probably different.

5. The greater the work-hardening rate, the greater the increase in difficulty of propagation as a function of reduction in thickness. This is probably because slip nuclei physically block the transformation interfaces, and the greater the work-hardening rate, the greater the total number of slip nuclei. Also, for small amounts of are postulated to enhance martensite nucleation, increases as the total number of slip nuclei increases.

6. For each sample orientation, one observes practically the same change in difficulty of propagation ($dT/dR_{A\rightarrow M}$ or $dT/dR_{M\rightarrow A}$) as a function of reduction in thickness. Therefore, it is probable that few deformation induced defects reduction in thickness ($\leqslant 5\%$), the greater the peak enhancement of martensite nucleation, the greater the difficulty of propagation, because the number of $\{110\}\langle 1\bar{1}0\rangle$ slip nuclei, which are erased by the transformation interface after two cycles.

7. Defect pinning of the interface is suggested as a possible mechanism for the increased difficulty of propagation, and the decreased degree of transformation, that is observed upon deformation.

Acknowledgements

The authors wish to thank F. J. DiSalvo, J. V. Waszczak and D. Dorsi for their excellent technical assistance. Stimulating discussions were held with S. Mahajan, G. Y. Chin and J. T. Plewes.

Appendix

That $\{110\}\langle 1\bar{1}0\rangle$ slip nuclei can be formed by the intersection of two $\{110\}\langle 001\rangle$ slip bands can be demonstrated through the following argument. Two $\{110\}\langle 001\rangle$ slip bands will intersect along a $\langle 111\rangle$ direction. The dislocations gliding on the two different systems that

TABLE IA

Compression axis	Systems activated*	Possible intersections	Line of intersection	New slip vector	New shear mode
[112]	A (110) [001]†	None	None	None	None
[110]	A (01$\bar{1}$) [100] B (10$\bar{1}$) [010]	A + B	[$\bar{1}\bar{1}\bar{1}$]	[110] [1$\bar{1}$0]	(1$\bar{1}$0) [110] ($\bar{1}\bar{1}$2) [1$\bar{1}$0]
[111]	A (011) [100] B (101) [010] C (110) [001]	A + B	[11$\bar{1}$]	[110] [1$\bar{1}$0]	(1$\bar{1}$0) [110] ($\bar{1}\bar{1}\bar{2}$) [1$\bar{1}$0]
		A + C	[111]	[101] [10$\bar{1}$]	(10$\bar{1}$) [101] ($\bar{1}\bar{2}\bar{1}$) [10$\bar{1}$]
		B + C	[$\bar{1}$11]	[011] [01$\bar{1}$]	(01$\bar{1}$) [011] ($\bar{2}\bar{1}\bar{1}$) [01$\bar{1}$]

*Based on Schmid factor analysis and slip trace observation.
†Not counting the two weak systems observed.

may be oriented along $\langle 111 \rangle$ can effectively combine to produce new $\langle 110 \rangle$ slip vectors. The resulting dislocation can glide in a plane containing $\langle 111 \rangle$ and the new slip vector. The following table lists the possible intersections between the slip systems that are activated in the samples used in this study, and the new shear modes that result from these intersections.

As an example, consider an intersection between slip systems A(011) [100] and C(110) [001] for the [111] sample. The glide planes intersect along $[\bar{1}1\bar{1}]$ and the two slip vectors can combine to yield the glide vectors [101] or $[10\bar{1}]$. The normals to the planes that these two new slip vectors can glide in are determined by the cross products $[101] \times [\bar{1}1\bar{1}]$ and $[10\bar{1}] \times [\bar{1}1\bar{1}]$ respectively. The combination of the new glide planes and the new slip vectors are the two new shear modes.

Note that not all intersections lead to $\{110\}\langle 1\bar{1}0 \rangle$ slip nuclei. However, the number of $\{110\}\langle 1\bar{1}0 \rangle$ slip nuclei produced is greater the greater the $\{110\}\langle 001 \rangle$ slip multiplicity. Presumably, the $\{112\}\langle 1\bar{1}0 \rangle$ shear mode does not enhance martensite nucleation because they are not the type of shear responsible for transformation.

References

1. E. SCHEIL, *Z. Anorg. Alleg. Chem.* **207** (1932) 21.
2. A. W. MCREYNOLDS, *J. Appl. Phys.* **20** (1949) 896.
3. E. S. MACHLIN and M. COHEN, *Trans. Met. Soc. AIME* **191** (1951) 746.
4. S. C. DAS GUPTA and S. S. PANI, *Trans. Indian Inst. Met.* **7** (1953) 161.
5. L. C. CHANG and T. A. READ, *Trans. Met. Soc. AIME* **191** (1951) 47.
6. M. W. BURKART and T. A. READ, *ibid* **197** (1953) 1516.
7. R. E. HUMMEL, J. W. KOGER, and V. PASUPATHI, *ibid* **242** (1968) 249.
8. W. A. RACHINGER and A. H. COTTRELL, *Acta Metallurgica* **4** (1956) 109.
9. N. NAKANISHI, Y. MURAKAMI, S. KACHI, T. MORI, and S. MIURA, *Phys. Letters* **37A** (1971) 61.
10. H. G. VAN BUEREN, *Phillips Res. Rep.* **12** (1957) 190.
11. P. M. ROBINSON and M. B. BEVER, *Acta Metallurgica* **13** (1965) 647.
12. A. J. BOGERS, *ibid* **10** (1962) 260.
13. J. F. BREEDIS and W. D. ROBERTSON, *ibid* **11** (1963) 547.
14. J. C. BOKROS and E. R. PARKER, *ibid* **11** (1963) 1291.
15. A. J. BOGERS and W. G. BURGERS, *ibid* **12** (1964) 255.
16. R. LAGNEBORG, *ibid* **12** (1964) 823.
17. W. G. BURGERS and J. A. KLOSTERMANN, *ibid* **13** (1965) 568.
18. K. MUKHERJEE and P. FERRAGLIO, *Fizika Suppl. No. 2*, (1970) 27. 1.

Received 16 April and accepted 11 June 1973.